

A Finite-Element Tool for Scattering from Localized Inhomogeneities and Submerged Elastic Structures

Mario Zampolli, David S. Burnett, Finn B. Jensen, Alessandra Tesei^{*},
Henrik Schmidt[†] and John B. Blottman III^{**}

^{}NATO Undersea Research Centre, 19138 La Spezia, Italy*

[†]Department of Ocean Engineering, Massachusetts Institute of Technology, Cambridge, MA 02139

*^{**}Naval Undersea Warfare Center, Division Newport, Code 2131, Newport, RI 02841-1708*

Abstract. A steady-state 3-D finite-element tool called FESTA (Finite-Element STructural Acoustics), is being developed at the NATO Undersea Research Centre. The code is geared towards a variety of applications in underwater acoustics, such as multistatic scattering from localized inhomogeneities, scattering across interfaces between fluids and/or solids, and multistatic scattering from single and multiple fluid-loaded elastic targets. The hp-adaptive finite-element technology used to develop FESTA allows the user to optimize the convergence as well as the demand on computing resources by selectively changing the element size (h-refinement) and/or by increasing the order of the polynomial finite-element shape functions (p-enrichment). An efficient hybrid tool for the computation of multistatic scattering from targets buried, partially buried or proud inside shallow water waveguides is being developed in conjunction with MIT. In this hybrid tool FESTA is used to perform target computations in the near field of the scatterer, while the waveguide propagation model OASES computes the far field propagation of the incident and scattered acoustic fields. The presentation focuses on the most relevant details of the formulations implemented in FESTA, as well as on application examples for frequencies ranging from 1 kHz to a few tens of kHz.

INTRODUCTION

The steady-state **Finite Element STructural Acoustics** code called **FESTA**, which is under development at the NATO Undersea Research Centre, is based on a fully 3-D continuum mechanics description of the acoustics in both fluid and elastic media. The basic building block for the tool is a state-of-the-art commercial finite element kernel and library called ProPHLEX, which is developed at COMCO/Altair Engineering (see [1]). FESTA is capable of computing efficiently the multistatic scattered field in the vicinity of localized inhomogeneities and/or of elastic objects with internal structure, such as mines. Because of the computational cost associated with 3-D finite element computations, one is usually limited to finite element domains which are not larger than at most a few tens of wavelengths. Common problems of scattering from objects in underwater waveguides, on the other hand, require the computation of the acoustic field in much larger domains. To overcome this limitation, FESTA has been interfaced with the MIT wavenumber integration propagation tool OASES [2, 3]. The resulting hybrid FESTA/OASES tool is capable of treating 3-D elastic objects of arbitrary shape inside ocean waveguides. This paper focuses on the technique developed to couple FESTA

with OASES by giving a brief description of the relevant mathematical formulations. Several applications of FESTA and of the hybrid tool are discussed in the oral conference presentation.

THEORY

This section describes briefly the steady-state structural acoustics equations used in FESTA, and the boundary conditions implemented in the current version of the tool. A special boundary condition which is used to couple FESTA with underwater propagation tools is also presented. For a more detailed discussion of the derivations and theory underlying FESTA, the reader is referred to [4, 5].

Assuming $\exp(+i\omega t)$ time-dependence, where ω is the angular frequency and t represents time, the linear wave equations for an anisotropic elastic solid in a cartesian coordinate system can be written as:

$$(c_{\alpha l \beta m} u_{\beta, m})_{, l} + \omega^2 \rho^s u_{\alpha} = 0, \quad (1)$$

with $\alpha, \beta = 1, \dots, 6$, and with the latin indices $l, m = 1, 2, 3$ representing the cartesian coordinates x, y and z . The displacement vector in the solid is:

$$(u_1, \dots, u_6) = (u_x^R, u_y^R, u_z^R, u_x^I, u_y^I, u_z^I), \quad (2)$$

where (u_x, u_y, u_z) is the complex displacement vector in cartesian coordinates, and the superscripts R and I denote the real and imaginary parts, respectively. According to the definitions of tensor calculus, repeated indices in a term imply summation, and a comma preceding a subscript index denotes differentiation with respect to the coordinate associated with the index. The material properties in equation (1) are given by the tensor of elastic moduli $c_{\alpha l \beta m}$ and by the density ρ^s . In its most general form, $c_{\alpha l \beta m}$ can describe fully anisotropic elastic materials.

The complex pressure $p = (p^R, p^I)$ in the fluid is described by the Helmholtz equation

$$\left(\frac{1}{\omega^2 \rho^f} p_{\alpha, m} \right)_{, m} + K_{\alpha \beta} p_{\beta} = 0. \quad (3)$$

The material properties of the fluid are the density ρ^f and the compressibility matrix

$$[K] = \frac{1}{B^R(1 + \delta^2)} \begin{bmatrix} 1 & -\delta \\ \delta & 1 \end{bmatrix}, \quad (4)$$

where B^R is the dynamic bulk modulus, and δ is the damping factor. Although the writing of complex equations as systems of purely real equations may seem somewhat awkward to the reader, the reason motivating this choice in the present paper is that the ProPHLEX FE development library and kernel used by the authors requires all quantities to be purely real (see [1]).

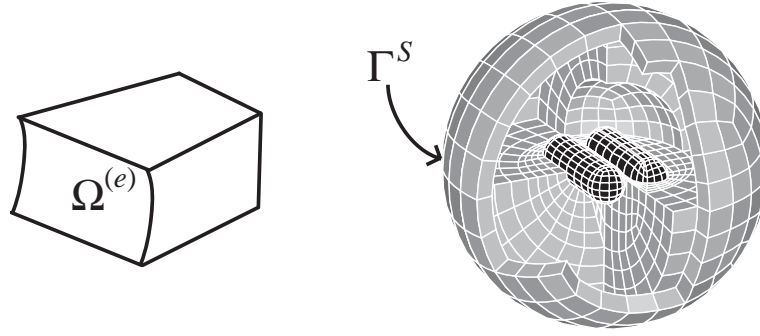


FIGURE 1. A generic finite element $\Omega^{(e)}$, and a view into a 3-D finite element mesh of two hollow steel cylinders (black elements) surrounded by a ball of fluid elements. The ball of fluid is bounded by the spherical surface Γ^S , on which radiation conditions are applied to ensure the outward radiation of the scattered field.

Finite element equations

Instead of deriving separate finite element equations for a solid element and for a fluid element, one can construct a single type of finite element which represents either a solid or a fluid, depending on the choice adopted for the constants in the equations. Figure 1 shows an example of a single element and of a full finite element mesh consisting of approximately 2000 elements, some of which are solid elements (two cylinders in the center of the mesh), while the others are fluid elements. The first step in writing a single FE equation for the two media is to group equations (1) and (3) into one single expression:

$$(a_{\alpha l \beta m} q_{\beta, m})_{,l} + c_{\alpha \beta} q_{\beta} = 0, \quad (5)$$

with $\alpha, \beta = 1, \dots, 8$. The unknown vector quantity $\{q\}$ is defined by

$$\{q\} = \{u_x^R, u_y^R, u_z^R, u_x^I, u_y^I, u_z^I, p^R, p^I\}^T, \quad (6)$$

where the superscript T denotes the transpose. The wave equation for a solid is obtained from equation (5) by choosing

$$a_{\alpha l \beta m} = \begin{cases} c_{\alpha l \beta m} & \alpha, \beta = 1, \dots, 6 \\ 0 & \text{otherwise} \end{cases} \quad (7)$$

$$c_{\alpha \beta} = \begin{cases} \omega^2 \rho^s \delta_{\alpha \beta} & \alpha, \beta = 1, \dots, 6 \\ 0 & \text{otherwise.} \end{cases} \quad (8)$$

The symbol $\delta_{\alpha \beta}$ represents the Kronecker Delta, which is equal to unity if and only if $\alpha = \beta$, while it is zero for $\alpha \neq \beta$. The equations for a fluid are obtained easily from (5) by setting

$$a_{\alpha l \beta m} = \begin{cases} \frac{\delta_{\alpha \beta} \delta_{lm}}{\omega^2 \rho^f} & \alpha, \beta = 7, 8 \\ 0 & \text{otherwise} \end{cases} \quad (9)$$

$$c_{\alpha \beta} = \begin{cases} K_{\alpha \beta} & \alpha, \beta = 7, 8 \\ 0 & \text{otherwise.} \end{cases} \quad (10)$$

The starting point for the derivation of the Bubnov-Galerkin integral equations for a generic fluid/solid element is the expansion of each of the 8 field variables q_β in a series of v basis functions,

$$q_\beta = \Phi_{\beta j} Q_j, \quad \beta = 1, \dots, 8; j = 1, \dots, 8v. \quad (11)$$

The basis functions, which in the present case are the hierarchic polynomials defined in [1], are grouped into the matrix

$$[\Phi] = [\phi_1[I], \dots, \phi_v[I]], \quad (12)$$

where $[I]$ is an 8×8 identity matrix. The vector Q_j contains the unknowns, which are the coefficients of each individual basis function.

Equation (5) is premultiplied by $[\Phi]^T$ and integrated over the element volume $\Omega^{(e)}$. Application of the divergence theorem and the substitution of Eq. (11) into the $a_{\alpha l \beta m}$ and $c_{\alpha \beta}$ integrals yields the finite element linear matrix equation

$$\left[\int_{\Omega^{(e)}} \Phi_{i\alpha} a_{\alpha l \beta m} \Phi_{\beta j, m} d\Omega - \int_{\Omega^{(e)}} \Phi_{i\alpha} c_{\alpha \beta} \Phi_{\beta j} d\Omega \right] Q_j = \underbrace{\int_{\partial\Omega^{(e)}} \Phi_{i\alpha} a_{\alpha l \beta m} q_{\beta, m} n_l d\Gamma}_{I_{\partial\Omega^{(e)}}}, \quad i = 1, \dots, 8v, \quad (13)$$

where $\partial\Omega^{(e)}$ represents the boundary of the element (e). The vector n_l is the unit normal on $\partial\Omega^{(e)}$ pointing outward. The boundary conditions on the faces of an element are applied via the integral $I_{\partial\Omega^{(e)}}$.

Once the computational domain has been divided into a mesh of elements, the linear equations (13) corresponding to each element are assembled into a global sparse linear system of equations. Assembly enforces the inter-element continuity of normal particle displacement within the solid domain and the inter-element continuity of acoustic pressure inside the fluid domain.

For any pair of adjacent fluid elements, the assembly process also produces a difference of two $I_{\partial\Omega^{(e)}}$ integrals on the interface shared by each of the two elements. Since $a_{\alpha l \beta m} q_{\beta, m} n_l$ represents the normal particle displacement, which is required to be continuous across the interface between two adjacent elements, the difference of two $I_{\partial\Omega^{(e)}}$ integrals is set to zero. Similarly, the difference of two $I_{\partial\Omega^{(e)}}$ integrals on the interface between two adjacent solid elements is set to zero because $a_{\alpha l \beta m} q_{\beta, m} n_l$ represents the normal component of the stress tensor, which also has to be continuous. The continuity of normal stress and displacement cannot be imposed naturally by the assembly process across the interface between a fluid and a solid element. To join the solid and the fluid domains, the continuity of normal stress and particle displacement on the common interfaces between adjacent solid and fluid elements is guaranteed by solid/fluid coupling surface integrals, which convert the solid degrees of freedom to compatible fluid degrees of freedom and vice-versa. Other boundary conditions which can be applied to the finite element equation are the Dirichlet, Neumann, and Mixed conditions on the free faces of an element. To apply the Sommerfeld radiation condition for unbounded domains in

an approximate form, the Bayliss-Turkel first order radiation conditions (see [6]) are used on the free faces of a spherical surface enclosing the finite element computational domain. The reader is referred to [4, 5] for a more detailed discussion of the boundary conditions implemented in FESTA.

Hybrid finite element/propagation tool modeling

In many practical applications it is necessary to compute the acoustic field inside a shallow water waveguide containing one or more targets. For such problems, the size of the overall computational domain is usually around a few hundreds of wavelengths in range and depth, while the size of the target is on the order of one to a few tens of wavelengths. Experience shows that the complete solution of such problems by the finite element technique alone is not feasible because of the computational cost associated with 3-D FE codes. On the other hand, many underwater propagation tools, such as OASES/SAFARI [2, 3], compute the propagation inside ocean waveguides efficiently, but lack the capability of treating arbitrarily shaped 3-D elastic targets. These different characteristics of the FE technique and the propagation tools suggest that the 3-D scattering problems in underwater ducts can be solved by a technique in which the finite element tool and a propagation code are interfaced to form a hybrid tool. The hybrid technique presented here is based on the decomposition of the problem into a long-range propagation sub-problem, which can be solved by the propagation tool, and a nearfield scattering sub-problem to be solved by the finite element tool. The boundary data required for the definition of the local finite element scattering problem is assigned via the boundary condition presented below.

The communication between the finite element model and the wavenumber integration tool occurs through the three step procedure outlined in Fig. 2. In the first step, the propagation tool computes the acoustic field inside the shallow water waveguide in absence of the target. In the second step, the incident field computed in step one and its normal derivative are assigned on Γ^S (see figure 1) as incident field data for the local scattering computation. An approximate form of the Sommerfeld radiation condition to ensure the outward radiation of the scattered field is also needed on Γ^S . At this point, the finite element scattering problem is solved by FESTA, and the total field resulting from the computation is sampled on the boundary of the sphere. Subtraction of the incident field from the FESTA result yields the scattered field on Γ^S . In the third and last step, the scattered field and its normal derivative are passed back to the propagation tool, which constructs a multipole having the same radiation pattern as the scattered field. The multipole is then used as a source for the propagation of the scattered field through the underwater channel.

The boundary conditions for coupling FESTA to the propagation tool in step two are obtained from the boundary integral $I_{\partial\Omega^{(e)}}$ in Eq. (13). To achieve this, the boundary integral for a fluid is expressed explicitly in terms of the gradient of the acoustic pressure as

$$I_{\partial\Omega^{(e)}} = \int_{\Gamma^S} \frac{1}{\omega^2 \rho_f} \Phi_{i\beta} p_{\beta, l} n_l d\Gamma, \quad (14)$$

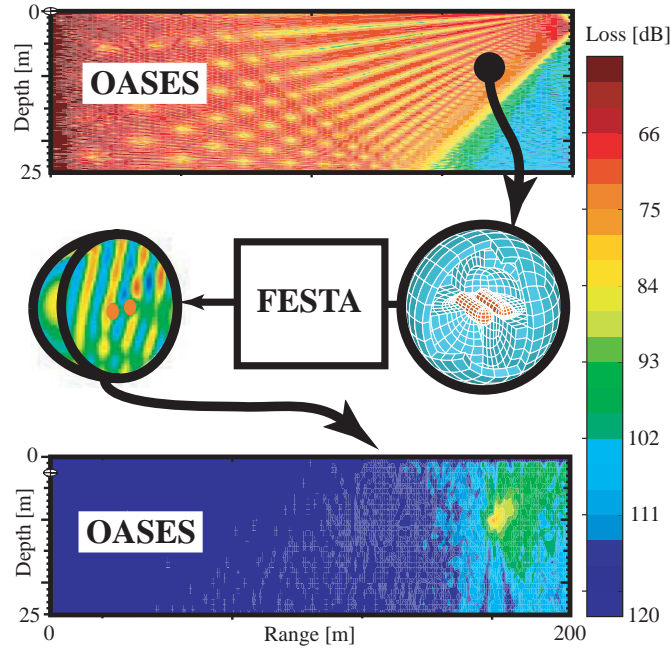


FIGURE 2. Example of a coupled FESTA/OASES computation. Step 1: incident field computation with OASES. Step 2: scattered field computation with FESTA, using the incident field from step 1 as a BC on the spherical surface Γ^S . Step 3: the scattered field is propagated in the waveguide by OASES.

with $\beta = 1, 2$. Denoting the incident field by p_β^{inc} and the scattered field by p_β^{scat} , the total pressure p_β can be written as

$$p_\beta = p_\beta^{\text{inc}} + p_\beta^{\text{scat}}. \quad (15)$$

The approximate radiation condition for the scattered field used here is the one developed by Bayliss, Turkel and co-workers ([6]):

$$\frac{1}{\rho f} p_{\beta,l}^{\text{scat}} n_l = R_{\beta\alpha} p_\alpha^{\text{scat}}, \quad \alpha = 1, 2, \quad (16)$$

where the matrix $R_{\beta\alpha}$ represents the first order linear Bayliss-Turkel radiation operator. Substitution of equation (15) into equation (14) and application of the radiation condition (16) yield after some simple manipulation:

$$I_{\partial\Omega^{(e)}} = \int_{\Gamma^S} \frac{\Phi_{i\beta}}{\omega^2} R_{\beta\alpha} p_\alpha d\Gamma + \int_{\Gamma^S} \frac{\Phi_{i\beta}}{\omega^2} \left[\frac{1}{\rho f} p_{\beta,l}^{\text{inc}} n_l - R_{\beta\alpha} p_\alpha^{\text{inc}} \right] d\Gamma. \quad (17)$$

The first integral in equation (17) contains the unknown p_α and thus it is moved to the left-hand side of the FE linear equations. The other integral remains on the right-hand side of the FE system because it contains the incident field p_α^{inc} and its gradient, which are both computed by the propagation tool in the first step of the coupling procedure.

NUMERICAL RESULTS

To illustrate a possible use of the hybrid FESTA/OASES tool, an acoustic barrier for the detection of objects in shallow water is studied (Fig. 2). In the envisioned application, a focused field is generated in an area across which one wants to detect intruding foreign objects. The detection is based on the measurement of perturbations in the quiescent region below the focus, which are caused by the forward scattering from an object crossing the barrier.

The environment considered here is a Pekeris waveguide consisting of a 25m deep water layer with an infinite layer of sand below it. A vertical time-reversal mirror array, located at range 0m, focuses the emitted sound at range 200m, and at 2.5m depth. At the frequency of 10 kHz used in the computations, the area shown in Fig. 2 spans over 1300 wavelengths in range, and approximately 170 wavelengths in depth. The scatterers penetrating the focused acoustic field are two closely spaced void steel cylindrical shells with hemispherical endcaps, modeled with the mesh depicted in Fig. 1. Each cylinder has a diameter of approximately 18 cm (roughly 1 wavelength) and a length of 60 cm (4 wavelengths). A contour plot of the transmission loss against range and depth computed by OASES in the first step of the hybrid procedure, showing the unperturbed focused acoustic field inside the waveguide, is displayed in the top panel of Fig. 2. The acoustic field in the sediment is not plotted in the figure. In the second step of the computation, the targets are located at range 170m and at depth 20m (large dot in the figure), with the axes of the cylinders lying perpendicular to the range-depth plane shown in the figure, and with the centers of the cylinders aligned parallel to the bottom. The middle panel of the figure shows a representation of the FESTA computation, and the bottom panel shows the scattered field in the waveguide computed by OASES. The top arrow connecting OASES to FESTA and the bottom arrow connecting FESTA to OASES represent respectively the sampling of the incident field and of the scattered field on the surface Γ^S . On a high-end Unix RISC workstation, the typical CPU times for computations like the one shown here are on the order of one to a few hours for the FESTA step, and a few minutes for each of the two OASES steps.

CONCLUSIONS

The hybrid finite element scattering/wavenumber integration propagation technique presented makes it possible to address the problem of scattering from 3-D objects in shallow water environments. In the example shown above, the multiple scattering between the cylinders is treated properly by one single finite element computation because both cylinders belong to the same finite element mesh, on which the full acoustic wave equation is solved. The multiple scattering between the targets, the sea surface and the bottom, on the other hand, can be computed only by approximating the Born series of the scattering via multiple iterations of the described three-step procedure. Although the importance of multiple scattering effects is of lower order for situations like the one discussed above, the interactions between the targets and the sediment can dominate the scattering from partially buried or flush buried objects. To take such effects properly

into account, an environment-independent coupling technique based on the characterization of the target via in-vacuo response matrices is being investigated by the authors at the present time. The approach is based on the finite element analysis of the elastic responses of the target to a series of independent localized forces applied to its surface in the absence of a surrounding fluid. As a result of such computations, one obtains an admittance matrix in which the displacements and the forces on the surface of the target are related to each other. Using such a matrix as an input, OASES can rapidly compute the field scattered by the target for a given scenario, including the case of a partially or flush buried target. An alternate environment-independent coupling technique is obtained by considering an independent set of spherical harmonic fields incident on the target immersed in a fluid. For each different spherical harmonic case, a scattered field is computed, and the result is stored in a database. The scattering for a given incident field, like for example the focused field considered above, can be easily computed by decomposing the incident field into spherical harmonics, and by successively superimposing each spherical harmonic scattered field stored in the database according to the coefficients of the expansion. The common advantage associated with the environment-independent coupling techniques, is the capability to synthesize efficiently the scattered field for a given scenario by using a set of FE results which are calculated a priori, thus eliminating the need to repeat the computationally expensive finite element analyses for every single case considered.

ACKNOWLEDGMENTS

The collaboration of John Fawcett from DRDC Canada in the verification of cylinder scattering results with his thin shell FEM/BEM scattering tool is gratefully acknowledged. The authors are also grateful to Mark Stevenson and Reginald Hollett of the NATO Undersea Research Centre for the stimulating discussions on the focused field scattering problem.

REFERENCES

1. Liszka, T., Tworzydło, W., Bass, J., Sharma, S., Westermann, T., and Yavari, B., *Comput. Methods in Appl. Mech. and Engrg.*, **150**, 251–271 (1997).
2. Schmidt, H., OASES: User Guide and Reference Manual, Tech. rep., Dept. Ocean Engrg., MIT (1999), available via ftp: <ftp://keel.mit.edu/pub/Oases/oases.pdf>.
3. Schmidt, H., SAFARI: Seismo-acoustic fast field algorithm for range independent environments, Tech. Rep. SR-113, NATO Undersea Res. Ctr., La Spezia, Italy (1987).
4. Burnett, D. S., and Zampolli, M., Development of a finite-element, steady-state, 3-D acoustics code for target scattering, Tech. Rep. SR-379, NATO Undersea Res. Ctr., La Spezia, Italy (2003).
5. Burnett, D. S., “Finite-element methods for structural acoustics: physics, mathematics and modeling,” in *Proc. 10th Internat. Cong. on Sound and Vibration*, Stockholm, Sweden, 2003.
6. Bayliss, A., Gunzberger, M., and Turkel, E., *SIAM J. Appl. Math.*, **42**, 430–451 (1982).